Screening of different computational models for the preparation of sol–gel imprinted materials

Elmer-Rico E. Mojica

Journal of Molecular Modeling
Computational Chemistry - Life Science - Advanced Materials - New Methods

ISSN 1610-2940
Volume 19
Number 9

J Mol Model (2013) 19:3911-3923
DOI 10.1007/s00894-013-1928-3

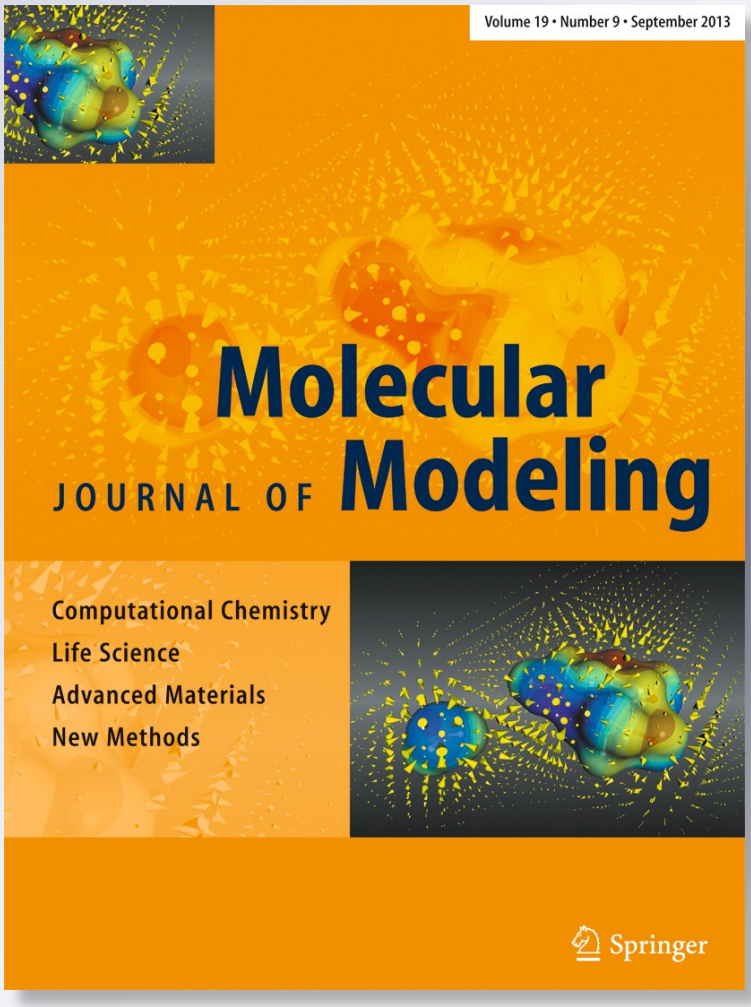

Springer

J Mol Model (2013) 19:3911–3923
DOI 10.1007/s00894-013-1928-3

ORIGINAL PAPER

Screening of different computational models for the preparation of sol–gel imprinted materials

Elmer-Rico E. Mojica

Received: 9 April 2013 / Accepted: 17 June 2013 / Published online: 6 July 2013

Abstract Different computational models were used and screened to find a rational way in selecting the appropriate functional silane monomer for the best molecular imprinted xerogel (MIX) formulation. Several functional silane monomers were used and allowed to react with a template model, tetracycline (TC). The resulting template-monomer complex molecules were first optimized and their interaction energies (IEs) were calculated using different computational methods such as semi-empirical methods, ab-initio methods, density functional theory (DFT) methods and solvent model method. The formulations used for calculation were also prepared and their performance in binding with TC was determined using tritium labeled sample. Results showed that the rankings of the different formulations varied with the different computational methods. However, rankings of the IEs of the xerogels are similar to that of the imprinting factor (IF) when HF and B3LYP at SV(P) and SVP basis set levels were used. The best imprinted xerogel, allyltriethoxysilane (AtEOS) ranked first in ten out of the 26 computational models that were screened and at all computational methods at tetramer system.

Keywords Computational · Imprinting · Sol–gel · Xerogel

Introduction

Molecular imprinting is a technology that allows the creation of polymeric materials with predetermined specificity. The resulting molecularly imprinted polymers (MIPs) exhibit dual characteristics of stability and robustness of synthetic polymers and recognition capabilities of biological receptors. These materials have been used in the separation sciences [1], sensor design [2], drug design [3] and catalysis [4]. It has also been used as sorbents in solid phase extraction (SPE) in complex sample analysis [5–7].

In general, the synthesis of MIP can be summarized as follows. First, the template and the functional monomer are mixed to form a complex in prepolymerization. The initiator and the crosslinker reagent is then added into the mixture and polymerization is carried out in the presence of heat or by UV treatment. Removal of the template after polymerization results in the formation of cavities which are complementary in both size and functionality with the target analyte. The success of molecular imprinting depends on the choice of the functional monomer used in the synthesis of MIP. It is crucial to know the interactions involved in the template-monomer complex. Optimizations are usually done using different formulations containing various functional monomers or in a trial-and-error fashion. This is time consuming and sometimes the ideal polymer is not obtained right away.

One approach that was adapted in order to better understand the intermolecular interactions during molecular imprinting is by using computational modeling for the rational design of the MIPs. The recent increase in computing power and the concurrent establishment of new and improved softwares has made the use of simulations based upon mathematical descriptions possible. Computer-aided design of MIP, which has emerged for several years, is now widely used.

The earliest attempt in using a computational approach was performed by Nicholls [8] who studied thermodynamic considerations of MIP recognition. Takeuchi et al. [9] then used Monte-Carlo-based technique to estimate the best possible complex structure based on the functional monomer-template conformation before polymerization. The Piletsky group used a virtual library of functional monomers to screen against the template molecules. The best monomer for the template was selected by comparing the binding energies of each virtual pair of monomer and template [10–13].

E.-R. E. Mojica (✉)
Department of Chemistry and Physical Sciences, Pace University, One Pace Plaza, New York, NY 10038, USA
e-mail: emojica@pace.edu

The Pavel group utilized state-of-the-art computational tools to achieve an understanding of intermolecular interactions in molecular systems that are employed in the imprinting of theophylline and its derivatives and chemical warfare agents into complex and monomeric systems [14–16]. Another research group developed a general strategy based on density functional theory (DFT) for the rational design of MIPs that permits the selection of the functional monomer and polymerization solvent [17, 18]. This method made use of the stabilization energies of the prepolymerization adducts between a selected template and different functional monomers and the effect of the polymerization solvent.

There are other studies which used the DFT to study the relationship between a template molecule and functional monomers [19, 20]. There are also studies which made use of the semi-empirical approach [21, 22]. The Regan group used Hyperchem to elucidate nature of non-covalent interactions present during the formation of the pre-polymerization complex [23] and to analyze whether or not it is possible to predict how well a given MIP will perform under set conditions [24] while another research group studied the molecular level properties of MIP using MMFF94 force field [25–27]. For the sol–gel based sorbents, Azenha et al. [28] applied the molecular modeling using the template-monomer interaction to predict the properties of the resulting molecular imprinted xerogels (MIX).

Although there is no general consensus of which computational model is most effective in determining the properties of the resulting MIP/MIX, the computational approach can help as a guide in determining the right functional monomers for a given template. The computational approach is a fast and no-reagent-consuming way to prepare the MIP/MIX. This can improve the trial and error approach commonly used by reducing both the expenses involved in preparing different formulations and the time utilized in determining the best formulation of sol–gel imprinted materials.

In this paper, several computational models were used to determine the IE of a model template, tetracycline, with different functional silane monomers. The main objective of this study is to screen computational models of different theoretical levels and to determine if there is a computational model that can correlate or predict the best functional silane monomer in terms of high selectivity and rebinding capacity.

Computational details

The summary on the use of computational models of different levels is shown in Fig. 1. Calculations were performed using Spartan [29] and Gaussian'03 [30] similar to what was previously reported [31]. Initially, the template and each silane monomer was subjected to a conformational search using the Spartan software package at a fast semi-empirical quantum mechanical level of theory using the PM3 Hamiltonian. The lowest-energy conformer was then further optimized at the Hartree-Fock (HF) level of theory by using several Gaussian-type basis sets (e.g., 3-21G, 6–31g(d), SV(P), and SVP). For each basis set, the silane monomer precursor and TC template lowest energies are given by $E_{monomer}$ and $E_{template}$, respectively.

For the dimer (silane monomer+template), trimer (silane monomer+crosslinker [tetramethoxysilane(TMOS)/tetraethoxysilane(TEOS)]+template) and tetramer (silane monomers+template+end capping agent (trimethychlorosilane [TMCS]) complexes, an initial conformational search was performed using a molecular mechanics force field (MMF94) [32] implemented in the Spartan software [29]. The ten most stable conformations were then subjected to additional geometry optimization by using the PM3 semi-empirical Hamiltonian. Of these ten initial conformations, the three geometries with the lowest PM3 energies were further optimized by using HF with different Gaussian-type basis sets (3-21G, SV(P), and SVP). Optimizations using the B3LYP density functional method were also performed to check that comparable structures were obtained with a correlated first-principles theoretical method. Another semi-empirical method, AM1, was also used to optimize the complex molecules in some instances. In each level, the structure with the lowest energy was used to compute for IE.

$$IE = E_{template:silane\ monomer} - E_{template} - \Sigma E_{silane\ monomer} \quad (1)$$

The simulation on the solvent effects was also done using conductor like screening model (COSMO). Geometry optimized structures of silanes, template and complex molecules by HF SV(P) were used to determine the solvent effect. The dielectric constant of the solvents used for the COSMO calculations (acetonitrile, water, methanol, ethanol and tetrahydrofuran) was used in the calculation for the solvent effect.

Comparison and correlation with experimental imprinting factors

Six functional monomers namely allyltriethoxysilane (AtEOS), phenyltriethoxysilane (PhetEOS), cyanoethyltrimethoxysilane (CNEtEOS), ethyltrimethoxysilane (C2tMOS), *n*-pentyltriethoxysilnae (C5tEOS) and *n*-octyltriethoxysilane (C8tEOS) (all from Gelest) used in the calculation were mixed with a crosslinker (TEOS or TMOS) at 1:1 mol ratio to prepare the TC imprinted xerogel. The imprinting factor (IF) of the uncapped and end capped xerogels using methanol for the binding study was based on the earlier paper reported by our group. Comparison and correlation between the theoretical IEs and the experimental IFs were evaluated. For the tetramers, only the endcapped xerogels were included in the correlation.

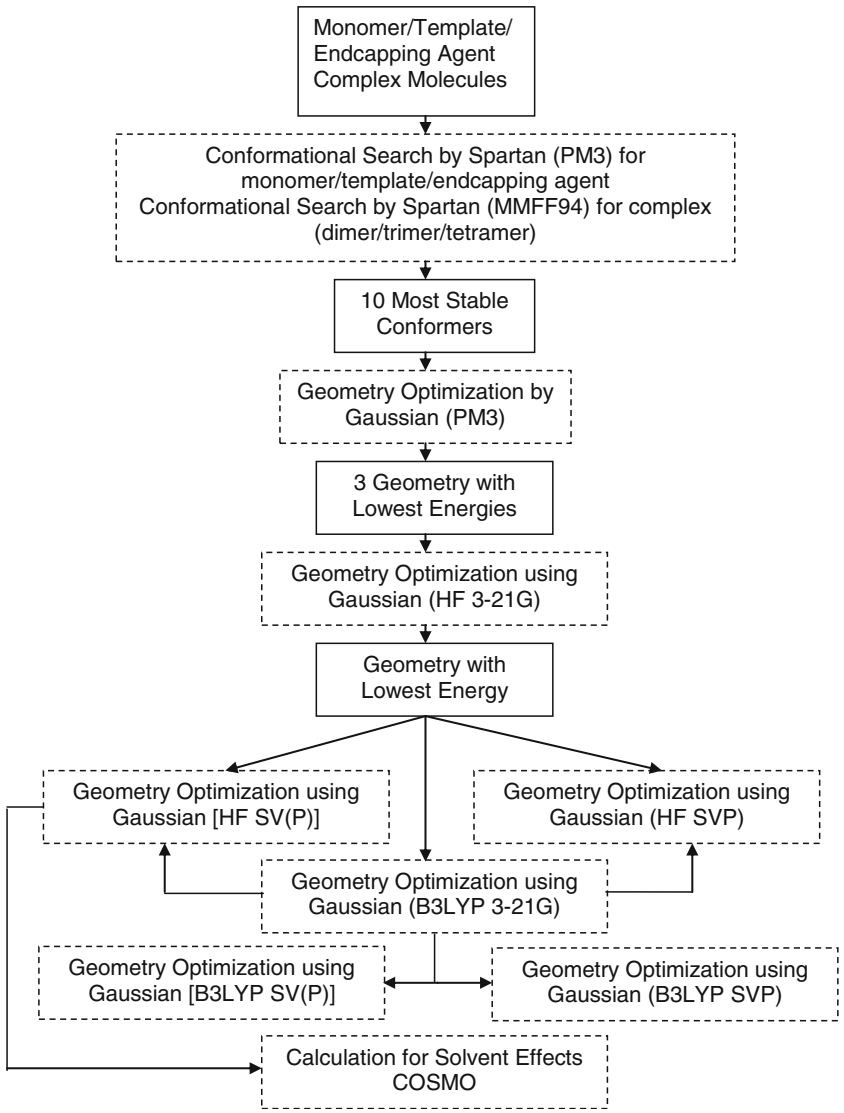

Fig. 1 Schematic of the computational models for calculation in this study

Results and discussion

The initial step in the MIX preparation, which is the formation of template-functional monomer complex, is similar to that in MIP synthesis. The monomer that can interact with the template most intensively will give the complex with the highest stability. This will facilitate the subsequent preparations including polymerization and the formation of the cavity which is a complementary structure to that of the template. The interaction of silane monomers with the template model, tetracycline, was determined first by obtaining the optimized minimal conformation of template-monomer complex and then calculating the IE for each template-monomer complex. Six silane monomers containing different functional groups were used. These functional groups include allyl, phenyl, cyano and alkyl chain groups represented by the ethyl, *n*-pentyl and *n*-octyl.

Conformations

Geometry optimization of conformers of template-monomer complex (dimer, trimer and tetramer) from conformational search initially performed in Spartan using MMFF optimization was performed. The optimized conformations of the six formulations (dimer) are shown in Fig. 2. Only the AtEOS and C2tMOS showed H-bonding interaction between the silane and the template. This is surprising since all silanes contain O and N (in the case of cyano) where an H-bond with the template can possibly form. The only possible explanation for this observation is due to the size of the functional group. The TC molecule contains an aromatic region, carbon backbone and various functional groups (double bonds, amine, carbonyl and hydroxyl) that can provide interaction sites (i.e., pi-pi interaction, H-bonding, dipole-dipole or hydrophobic interaction) with the silanes [31]. Both AtEOS and

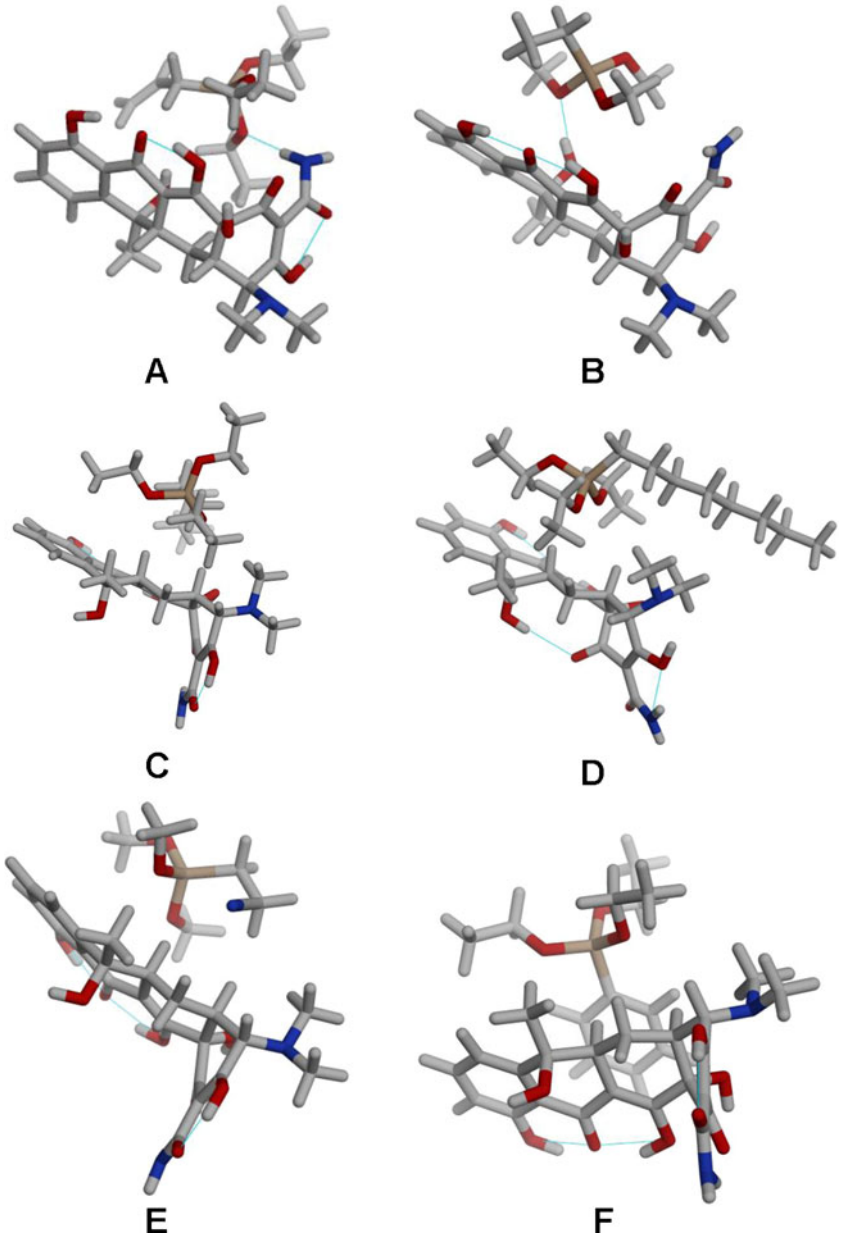

Fig. 2 Conformers with the lowest energy of dimers. **a** TC-AtEOS; **b** TC-C2tMOS; **c** TC-C5tEOS; **d** TC-C8tEOS; **e** TC-CNEtMOS and **f**: TC-PhetEOS

C2tMOS contain three or less carbon chains in the functional group in comparison to the other silanes. This small functional group may have allowed both silanes to form H-bonding with the template. The silanes with bigger or longer functional group may form a conformation that favored the other interactions aside from H-bond since TC contain different functional groups.

The optimized conformations of AtEOS formulation of different size (dimer, trimer and tetramer) are shown in Fig. 3. The silane monomer (AtEOS) is consistently on the same plane with respect to the template (TC) even with the addition of the crosslinker (TEOS) and the end capping reagent (TMCS). The optimized geometry of the complex has the template sandwiches in between the AtEOS and TEOS with TMCS. The allyl group of the silane interacts with the phenyl group of TC. However, the allyl group moves toward the amine group of TC with the addition of TEOS (trimer system). Addition of TMCS (tetramer system) results in the allyl group being closer to the phenyl group similar in the dimer system. The H-bond interaction is exhibited by the amine and hydroxyl group of TC with the oxygen of the methoxy group of AtEOS and TEOS. For the trimer and tetramer, the H-bond interaction is between the hydroxyl group of TC with the oxygen of a methoxy group of AtEOS.

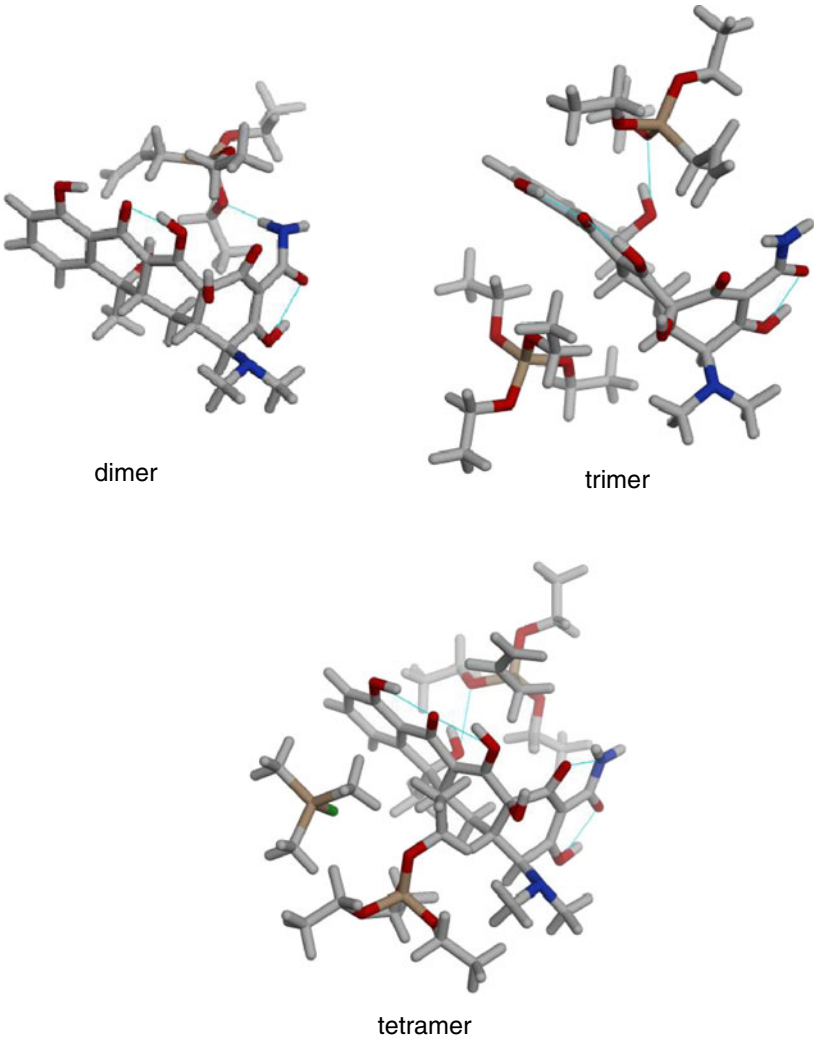

Fig. 3 Conformers with the lowest energy for a dimer (TC and AtEOS), a trimer (TC, AtEOS and TEOS) and a tetramer (TC, AtEOS, TEOS and TMCS)

Interaction energies and levels of computations

The IE between TC and the functional momoner was calculated using Eq. 1. It has been established that the higher the value of IE, the more stable the complex that will be formed between two chemical species. There are several levels of computations done in obtaining the IE. First, the IE of a template-functional monomer complex or dimer system was calculated. Next is the calculation of IE of a trimer system consisting of the dimer and a third species (either TEOS or TMOS) as the crosslinker. Another level of computation involved in the calculation of IE of a tetramer system wherein an end capping reagent (TMCS) was added to a trimer system. This addition of species has led to an increase in calculation time but it is necessary to simulate the condition where these species are present during the imprinting process. This is in addition to a longer calculation time already observed in MIX than MIP since silane monomers are larger species compared to acrylic monomers [28].

Geometry optimization using the different methods was ranked as semi-empirical < B3LYP < HF in terms of computational expenses. Semi-empirical calculations (PM3 and AM1) of silane monomers, template and the endcapping agent are completed within 10 min, and became longer when dimer (~10 h), trimer (~3 days) and tetramer (~7 days) were performed. For the HF and B3LYP calculations, the computational cost depends on the basis set used. The basis set 3-21G is the fastest with single molecule calculations completed ranging from 5 h to 10 h for both HF and B3LYP calculations. The time for completion ranges from 1–3 days for dimer calculation using both models. An additional day is needed for calculation to be completed using 6–31g(d). When SV(P) and SVP basis sets were used, computation was completed from 10–14 days. The SVP basis set has higher computational cost than SV(P) by just several hours. An additional 1–2 days was observed when HF calculation was performed. Calculations at trimer level further increase computational expenses to at least 20 days for B3LYP and at least 25 days for HF. Lastly, it takes at least

a month (~30 days) to complete tetramer level calculations for both HF and B3LYP.

Semi-empirical methods

Semi-empirical molecular orbital theory uses simplification of the Schrödinger equation $E\psi = H\psi$ to estimate the energy of a system (molecule) as a function of the geometry and electron distribution. The simplifications require empirically derived parameter ("fudge factors") to bring calculated values in agreement with the observed values. Semi-empirical methods are computationally fast because many of the difficult integrals are neglected. The error introduced is compensated through the use of parameters. The semi-empirical methods used namely PM3 and AM1, the more popular methods among the different semi-empirical methods due to availability of algorithms [33]. Both methods were already reported in the earlier studies for the calculation of interaction energies in MIPs [21, 34]. PM3 or parameterization method 3 and AM1 or Austin model 1 uses nearly the same equations with the PM3 having an improved set of parameters than AM1. PM3 is more accurate than AM1 for hydrogen bond angles but AM1 is more accurate for hydrogen bond energies [33].

Rankings of the different formulations as shown in Fig. 4 vary from one method to another and from size being calculated (dimer vs trimer vs tetramer). For instance, the ranking of the AtEOS formulation in PM3 improves with the addition of species from ranking last at dimer level improving to 2nd (trimer) and then to 1st at the tetramer level. For the AM1 (wherein the tetramer was not included), the ranking of the AtEOS formulation is 2nd in both the dimer and trimer level. The value of the calculated interaction energies in both empirical methods increases as the size of calculation increases except for CNEtMOS and C8tEOS formulations in PM3.

In addition, there is a difference in terms of the rankings of the different formulations in PM3 and AM1 in both dimer and trimer level. The observed inconsistency between PM3 and AM1 is in agreement with the essentially random character of the errors associated with semi-empirical methods and the intermolecular interactions being usually of the same magnitude [28]. Nevertheless, among the computational methods used, this is the least computationally demanding method getting results within a week.

Hartree-fock

Hartree-Fock is an ab-initio method that generates solutions to the Schrödinger equation where the real electron–electron interaction is replaced by an average interaction [35]. It is the simplest wavefunction based method involving optimization of a single optimization and its usefulness is limited because of complete neglect of electron correlation [36]. In large basis set, the HF wavefunction is able to account for ~99 % of the total energy but the remaining ~1 % is often very important for describing chemical phenomena [35]. The calculated IEs at the Hartree Fock (HF) level with different basis sets are shown in Fig. 5. At the 3-21G and 6–31g(d) basis set, the AtEOS is consistently within the three highest ranked monomer being first in the tetramer level. Most of the IE values increase with addition of chemical species in the system. At the SV(P) and the SVP levels, two tautomers of TC was used. It was found that after the B3LYP calculation, another structure or tautomer of TC was found to be more stable (Fig. 6). The tautomer predicted to be more stable at the B3LYP level (T2) has been reported as amongst the ten most stable by AM1/SCRF

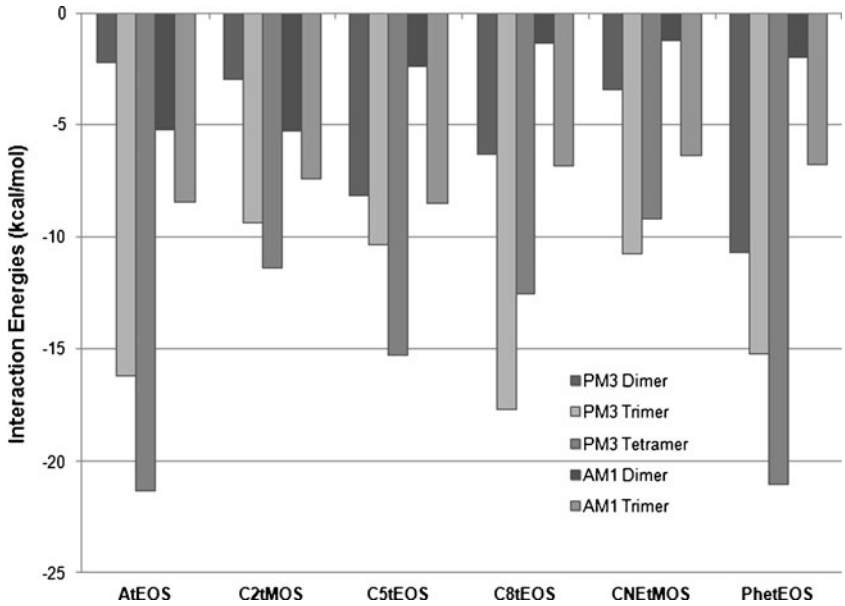

Fig. 4 Calculated interaction energies using semi-empirical methods (PM3 and AM1)

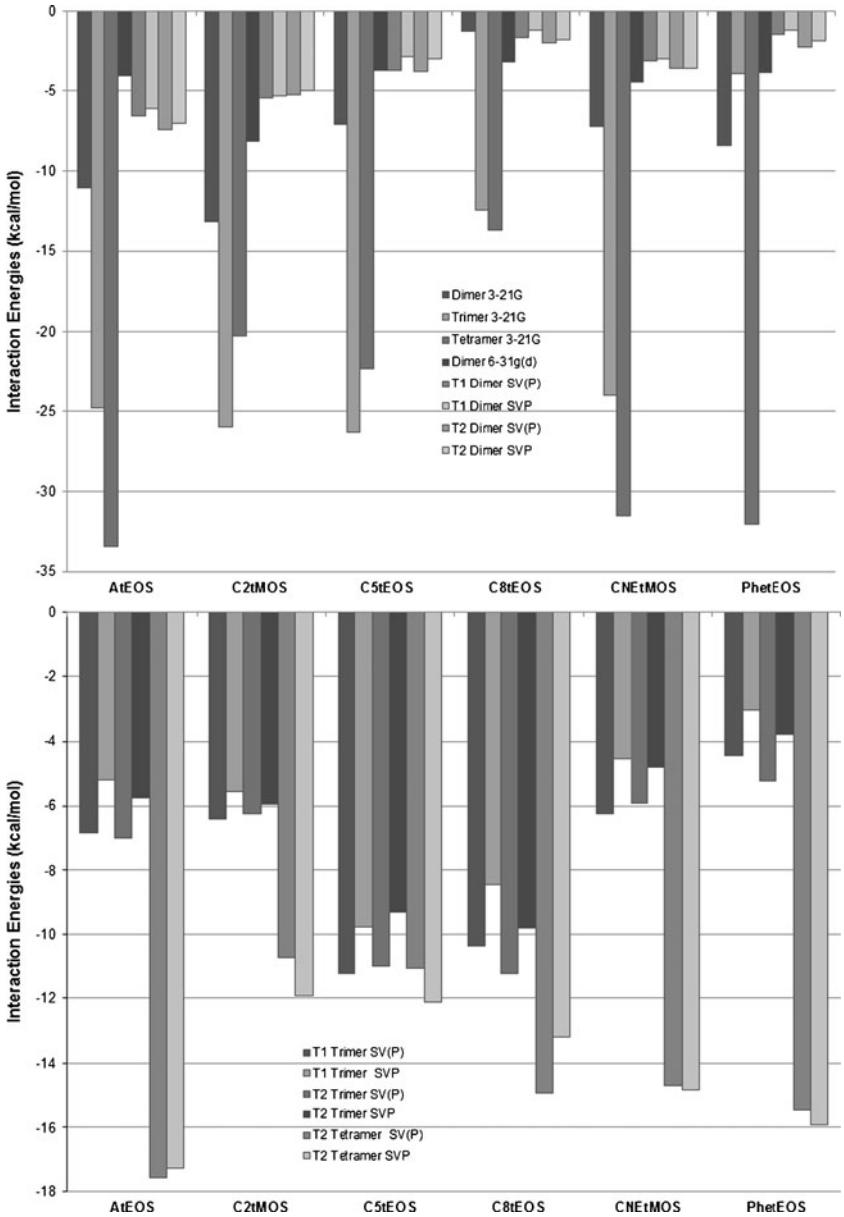

Fig. 5 Calculated interaction energies using HF in different basis sets

calculations [37]. Both tautomers (T1 and T2) were used for the calculation of IE to eliminate potentially missing effective interactions. The results are presented in Fig. 5. At these levels, the AtEOS and C2tMOS are constantly ranked first and second regardless of whatever tautomer was used. In addition, the C8tEOS and PhetEOS were consistently at the bottom of the rankings. The possible reason for this could be due to the size and nature of the functional group in the silanes. Both AtEOS

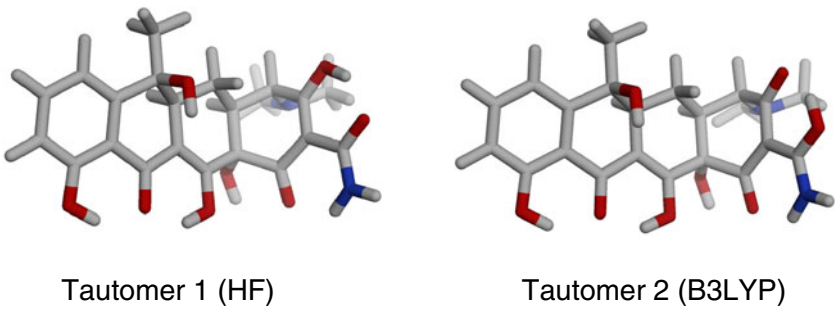

Fig. 6 TC tautomers observed during calculation

and C2tMOS contain shorter functional group compared to C8tEOS and PhetEOS. The higher ranked silanes are predicted to exhibit stronger interaction energies with the template since it is easier to reorient the smaller silanes to form the conformation that will favor H-bonding interaction with the template in comparison to the other silanes. It has been reported that the presence of multiple H-bonds results in a relatively large interaction energy [38].

Calculations at the HF levels for the trimers and tetramers are shown in Fig. 5. As in other basis sets and computational methods, the value of the IE increases as more species are added to the system with the exception of AtEOS. The observed IE value of AtEOS decreases from dimer to trimer level but have a big increase going to the tetramer level. In terms of rankings, the AtEOS formulation ranked 1st at the dimer level but dropped to as low as 4th at the trimer level. However, it is ranked at the top at the tetramer level.

B3LYP

Density functional theory (DFT) has become a standard method for electronic structure calculations in chemistry. The B3LYP (Becke, three parameter, Lee-Yang-Parr) method is a DFT based calculation containing a combined exchange functional and combined correlation functional and is widely used in chemical calculations because it leads to reliable results [39]. Figure 7 summarizes the calculations for IE at the B3LYP level. In terms of the values of IE, the B3LYP has higher values than those calculated using HF at the same basis sets. In terms of the size, there is an increase in the IE value from dimer to trimer level at the SV(P) and SVP basis sets. For the 3-21G basis set wherein a tetramer system was calculated, there is a linear relationship between the size and IE values except in AtEOS. The AtEOS formulation showed an initial decrease in IE value from dimer to trimer and then a drastic increase in the tetramer level. An unusual trend was observed in the rankings, wherein AtEOS ranked 1st or 2nd at the dimer level but drops to 6th ranked in trimer level. However, it ranked 1st at the tetramer level using 3-21G basis set. Calculations using the other basis sets at tetramer level were not performed because of time constraints.

The trend wherein the IE value or ranking of the monomer dropped by the trimer level has been observed using HF calculations. The interactions of the species involved can play an important role in the unusual trend observed. The change of AtEOS in rankings from dimer to tetramer levels in both HF and B3LYP can be explained by looking at the conformations observed at different size levels (Fig. 3). The position of the allyl group is different in the trimer system in comparison at the dimer or tetramer position. This can be one of the reasons why the value of IE or ranking of AtEOS suddenly dropped at the trimer level. It is also possible that the double bond of the allyl group contributes to this trend as the other formulation with double bond (PhetEOS) ranked also at 5th next to AtEOS at the trimer level.

The total interaction coming from H-bonding and pi-pi interactions could be the most important reason for the observed trend. There are different sites for H-bonding at the different size levels. H-bonding interaction is exhibited by the amine group of TC with the ethoxy group of AtEOS in the dimer level. At trimer level, the H-bond is between the hydroxyl group of TC and the ethoxy group. The H-bond is still between a hydroxyl group of TC and the ethoxy group at the tetramer level. On the other hand, pi-pi interaction could take place between the allyl group and the phenyl group. It is also observed that the allyl group of the silane interacts with the

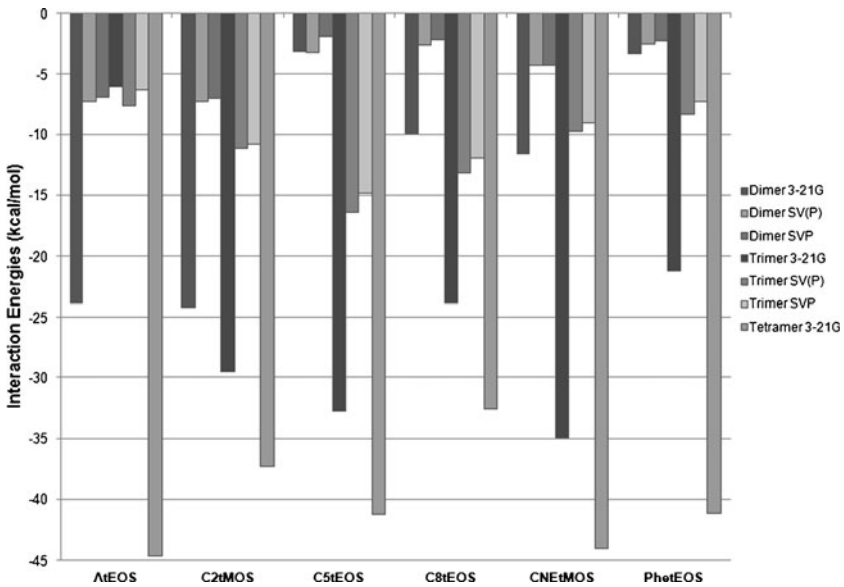

Fig. 7 Calculated interaction energies using B3LYP in different basis sets

phenyl group of TC at the dimer level. Addition of TEOS to the system pushed the allyl group toward the amine group of TC hence the allyl-phenyl interaction was not exhibited and this could be the main reason for the lower ranking of AtEOS at the trimer level. Lastly, the allyl group interacts with the phenyl group once again when TMCS was added at tetramer level. The large interaction energy could come from the additive effect of the H-bonding and pi-pi interactions exhibited by the different species in the system hence AtEOS ranked first at dimer and tetramer levels in both HF and B3LYP.

Literature has reported that the presence of H-bonds gives larger interaction energies in different computational methods. The resulting interaction energies from these H-bonds are not the same. In one study, H-bond interaction between harmane pyridinic nitrogen and hydroxyl group of metharcylic acid hydroxylic group is stronger than that between harmane pyrrolic group and carboxylic oxygen atom of methacrylic acid [40]. In addition, the presence of multiple H-bond interactions gives larger interaction energy [38].

Although B3LYP is less computationally expensive and more popular than HF, it has limitations in terms of interaction energy. Standard variants of DFT including B3LYP perform poorly in prediction of intermolecular interaction energies sometimes even giving wrong signs for these quantities. This is due to the self-interaction error cause by using approximate functional, i.e., inexact exchange in DFT calculations [41]. For instance, atomization energies using B3LYP has an average error of 3.11 kcal mol^{-1} which is a little bit better than that calculated using BLYP which gave an average error of 7.09 kcal mol^{-1} for the same data set [42]. This amount of error will significantly affect the value of interaction energies obtained from DFT-based calculations. This is the main reason why HF is preferred in this study than B3LYP although many still used DFT based calculations in terms of computational expense.

Solvent effect

The computational models discussed and considered so far are with respect to the gas phase. This condition is not observed in reality as the sol-gel process occurs inside a growing colloidal mixture that ultimately forms a gel. In this case the effect of solvent or solvation must be taken into account in energy calculations as it leads to changes in energy and stability of the functional monomer-template complexes. Solvent molecules can interact with the template and functional monomer in solvent environment. Solvents of various dielectric constants can influence the template-functional monomer interaction wherein the different dielectric constant could lead to different polarity of the solvents that can affect the conformation of the complex in a way that the recognition of the monomers with the template is different. The IE could reflect the effect of solvent on the complex formation.

There are two types of methods for evaluating the solvent effects: those describing the individual solvent molecules and those that treat the solvent as a continuous medium. The more popular continuum models such as polarizable continuum model (PCM) consider the solvent as a uniform polarizable medium with a dielectric constant of ε while the solute is placed in a suitable shaped cavity in the medium [43]. PCM has been used in the calculation of solvent effects in the preparation of MIPs [17, 44, 45].

In this case, another continuum model, conductor-like screening model or COSMO was used to calculate the solvent effect. COSMO takes into account the detailed atomic structure of the interface interacting with the dielectric liquid. It is a continuum method based on a solvent accessible surface and designed to be fast and robust as the method uses a simpler, more approximate equation for the electrostatic interaction between the solvent and solute. COSMO calculations requires shorter CPU time than PCM calculations and are less likely to fail to converge [33].

The interaction energies obtained at SV(P) level using the two tautomers with the different implicit solvents corresponded in every case to a significant decrease as compared to the gas-phase interaction. This makes sense since solvation of a species also involves intermolecular interactions of the same nature as functional monomer–template and so the solvent acts as a competitor. The intermolecular interaction between solvent molecules and the complex is competing with template-monomer interaction leading to weakening the interaction between the template and monomer [46]. It is also noticed that some of the monomers are not capable of forming interaction with template in some solvents because of the positive IE.

Results using the two tautomers showed that the best formulation in the different solvents tested is C2tMOS. It consistently ranks first in the different solvents. It has also been observed that the other straight chain alkoxysilanes (Tautomer 2 form) rank higher in most of the solvents. The ranking of the functional monomer with the highest IE at the gaseous state (AtEOS) ranges from second to fifth places in the solvents tested. Among the solvents tested, the tetrahydrofuran has the highest set of IE values in comparison to the other solvents. From the results shown in Fig. 8, it is concluded that type of solvent has a small influence on the complex stability.

Comparison of IE with IF

The performance of the prepared TC imprinted xerogels were determined by calculating their imprinting factor (IF). Table 1 summarizes the IF of the different xerogel formulations (uncapped and capped) using methanol as rebinding solvent. The AtEOS formulation has the highest IF in both the uncapped and capped xerogels. Capping the xerogel results in increased IF values in most xerogels. Although AtEOS ranks at

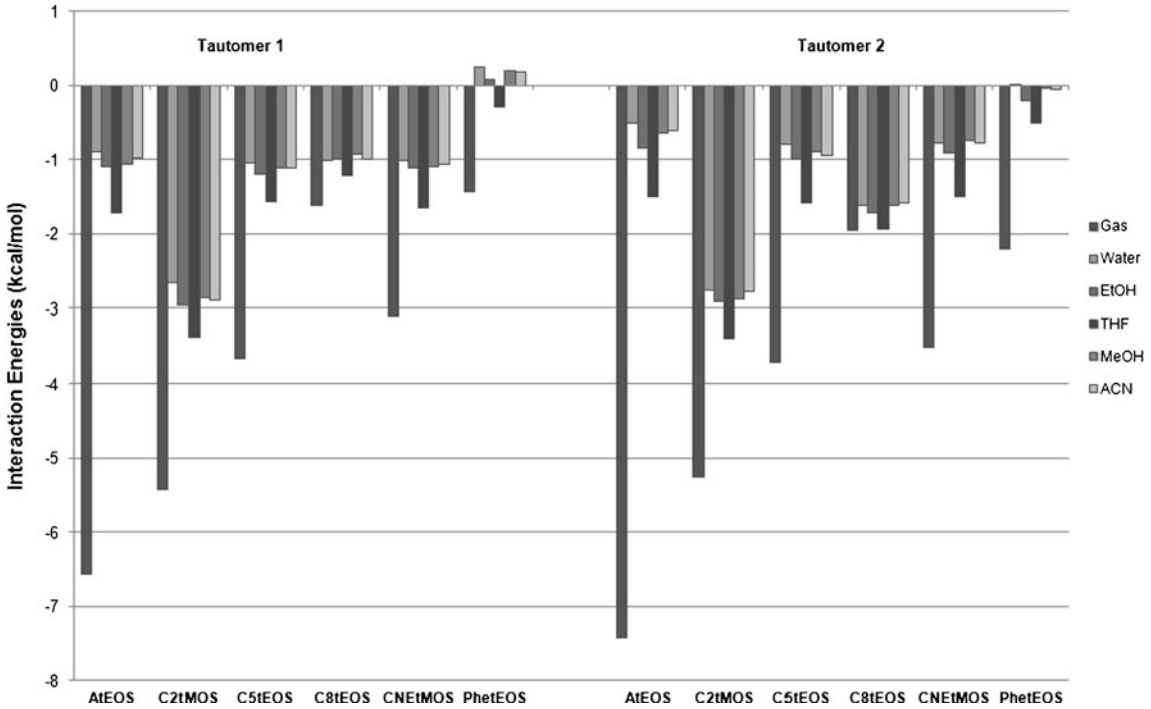

Fig. 8 Calculated interaction energies of the two tautomers (T1 and T2) of tetracycline using COSMO in HF SV(P) basis set

the top, the rankings of the other formulations are not the same in the uncapped and capped condition.

The success of a particular computational model lies in its ability to predict the binding performance of a MIX formulation with the calculated IE. It is assumed that during the imprinting process, the early TC-silane monomer(s) interactions govern the MIX performance. The more specific and stronger the interactions are, the better the so formed imprint will be for TC-binding. With this, the rankings of the different xerogel formulations in terms of theoretical IEs were compared with the experimental IFs.

Inspection of the different computational models consistently shows that the xerogel with the highest IF (AtEOS) also had the highest IE in ten out of the 26 models (COSMO not included) using different number of chemical species (dimer, trimer, tetramer). The C2tMOS formulation ranks first in six out of the 26 models screened and in all COSMO calculation. In all computational methods (semi-empirical, ab-initio and DFT), the AtEOS constantly ranks first at the tetramer level. In addition, AtEOS also ranks first at the dimer level using SV(P) and SVP basis sets (except at B3LYP SVP basis set). This could only mean that a semi-empirical method like PM3 can predict the best performing xerogel as long as it includes all the possible species present in the system.

Table 1 Imprinting factors and rankings () of xerogels using methanol as rebinding solvent

Xerogel	Uncapped	End capped
AtEOS	3.16 *(1)*	6.50 *(1)*
C2tMOS	2.50 *(4)*	4.75 *(2)*
C5tEOS	2.62 *(3)*	4.63 *(3)*
C8tEOS	3.21 *(6)*	3.71 *(4)*
CNEtMOS	3.05 *(2)*	3.22 *(5)*
PhetEOS	1.51 *(5)*	3.93 *(6)*

Several basic patterns have been observed in terms of the tautomers and basis sets [(SV(P) and SVP] used in calculations. In general, T2 have higher interaction energies than the T1 counterpart. The exception to this is C2tMOS [both dimer SV(P) and SVP and trimer SV(P)], CNEtMOS [trimer SV(P)] and C5tEOS [both trimer SV(P) and SVP]. In addition, calculations at both HF and B3LYP methods showed consistently higher values of interaction energies using SV(P) in comparison to SVP for the same tautomer and silane. The difference between the two basis sets is the absence of polarization functions of hydrogen in SV(P) compared to the more flexible SVP. These observations agreed with what was reported in an earlier paper [31].

In terms of the best computational model that shows almost the same ranking between the IEs and the IFs, the HF at SV(P) level (tautomer 2) predicts the correct ranking of four xerogels. Calculations using SV(P) and SVP basis sets at both HF and B3LYP tend to rank the better performing xerogels among the best MIXs in terms of IE. The correlation between IE vs. IF was also found to be not optimal with the highest r^2 value obtained to be only 0.76 at HF using SV(P)

basis set (dimer level) followed by 0.70 at the same computational method using SVP basis set. In one related study that made use of correlation, r^2 between 0.7 and 0.8 were reported, but r^2 dropped to 0.5 when one descriptor was excluded [47]. Thus, it is not surprising that the IF vs. IE r^2 values is mediocre given the uncertainties and complexities (*vide infra*).

The rankings of the xerogels at the HF SV(P) basis set level (dimer level) and the high correlation at this level only means that this is the best computational model among all models that have been screened. This computational level is close to what has already been used before in preparing MIPs. Computational design of polymer for aniline made use of HF method in MP2 level at 6-31++G(d) basis set [48]. In another study, HF/6-31G* was used to prepare MIPs for phenol [49] and a chiral, polymerizable metallodendrimers P2Pt(S-BINOL) [50].

The results of this study have several limitations as there are other factors that need to be considered. First and most importantly, sol–gel reactions occur in solvent with growing colloidal mixture that forms into a gel while all calculations were conducted in gas phase with one method using solvent effects. Although the calculations include as many of the reagent present, there are other species that are formed once the sol–gel process occurs. Among these are the hydrolyzed products coming from the silanes. The complex mechanisms involved in sol–gel process is very hard to simulate using commonly known computational models. It is possible that improvement on simulation or modeling can be done with the advent of new computational approaches such as quantum Monte Carlo or metadynamics. A study has been made using molecular dynamics to model the pregelification stage of the sol–gel process [51]. Another consideration is all interaction energies obtained are based on zero-temperature conformational optimizations and it is possible that at finite temperature, these interactions or configurations could be quite different. However, the use of different computational methods is still a better approach in preparing sol-gels for imprinting than the arbitrarily trial and error methods.

Conclusions

This work presents the screening of different computational models to find a rational approach in selecting the most suitable functional silane monomer in preparing molecular imprinted xerogels. The model template used, tetracycline, was allowed to interact with different functional silane monomers. The resulting template-monomer complex molecules were first optimized and their interaction energies (IE) (difference of complex molecules energy with the components) were obtained using different computational methods such as semi-empirical methods (PM3 and AM1), ab-initio methods (HF with different Gaussian type basis sets, i.e., 3-21G, SV(P) and SVP), density functional theory (DFT) method (B3LYP) and solvent model method (COSMO). Rankings from some computations agreed with the experimental data (IF). Increasing the number of chemical species being calculated increases the probability of predicting the best performing xerogels as confirmed with the results from tetramer level. A fast calculation using semi-empirical methods like PM3 was able to predict the best xerogel at the tetramer level. Computations at the SV(P) and SVP basis set at HF level also agreed with the experimental results. Overall, the results demonstrate the potential and limitations of using theoretical calculations to guide the development of analyte selective MIXs in comparison to arbitrary combinatorial methods like the trial and error approach.

Acknowledgments This material is based upon the work supported by the National Science Foundation (NSF) under Grant No. 0750321. Any opinions and conclusion or recommendations expressed in this material are those of the author and do not necessarily reflect the views of the NSF. The author thanks Diana Aga, Frank V. Bright and Jochen Autschbach of the Department of Chemistry, University at Buffalo for all the support they gave at the start of the project, Scott Simpson of the Department of Chemistry University at Buffalo and Ricky Nellas of the Oakridge National Laboratory for their comments on the paper. Support was also provided by the Center for Computational Research at the University at Buffalo. Molecular graphics images were produced using the UCSF Chimera package from the Resource for Biocomputing, Visualization, and Informatics at the University of California, San Francisco (supported by NIH P41 RR001081).

References

1. Haginaka J (2009) Molecularly imprinted polymers as affinity-based separation media for sample preparation. J Sep Sci 32:1548–1565
2. BelBruno JJ, Richter A, Gibson UJ (2008) Amazing pores: processing, morphology and functional states of molecularly imprinted polymers as sensor materials. Mol Cryst Liq Cryst 483:179–190
3. Alvarez-Lorenzo C, Concheiro A (2004) Molecularly imprinted polymers for drug delivery. J Chromatogr B 804:231–245
4. Tong KJ, Xiao S, Li SJ, Wang J (2008) Molecular recognition and catalysis by molecularly imprinted polymer catalysts: thermodynamic and kinetic surveys on the specific behaviors. J Inorg Organomet Polym Mater 18:426–433
5. Chapuisa F, Mullota JU, Pichona V, Tuffalb G, Hennion MC (2006) Molecularly imprinted polymers for the clean-up of a basic drug from environmental and biological samples. J Chromatogr A 135:127–134
6. Jing T, Gao XD, Wang P, Wang Y, Lin YF, Zong XC, Zhou YK, Mei SR (2007) Preparation of high selective molecularly imprinted polymers for tetracycline by precipitation polymerization. Chin Chem Lett 18:1535–1538
7. Schirmera C, Meisel H (2006) Synthesis of a molecularly imprinted polymer for the selective solid-phase extraction of chloramphenicol from honey. J Chromatogr A 1132:325–328
8. Nicholls IA (1995) Thermodynamic considerations for the design of and ligand recognition by molecularly imprinted polymers. Chem Lett 24:1035–1036
9. Takeuchi T, Dobashi A, Kimura K (2000) Molecular imprinting of biotin derivatives and its application to competitive binding assay using nonisotopic labeled ligands. Anal Chem 72:2418–2422
10. Chianella I, Karim K, Piletska EV, Preston C, Piletsky SA (2006) Computational design and synthesis of molecularly imprinted

polymers with high binding capacity for pharmaceutical applications-model case: adsorbent for abacavir. Anal Chim Acta 559:73–78
11. Chianella I, Lotierzo M, Piletsky SA, Tothill IE, Chen BN, Karim K, Turner APF (2002) Rational design of a polymer specific for microcystin-LR using a computational approach. Anal Chem 74:1288–1293
12. Piletsky SA, Karim K, Piletska EV, Day CJ, Freebairn KW, Legge C, Turner APF (2001) Recognition of ephedrine enantiomers by molecularly imprinted polymers designed using a computational approach. Analyst 126:1826–1830
13. Turner NW, Piletska EV, Karim K, Whitcombe M, Malecha M, Magan N, Baggiani C, Piletsky SA (2004) Effect of the solvent on recognition properties of molecularly imprinted polymer specific for ochratoxin A. Biosens Bioelectron 20:1060–1067
14. Pavel D, Lagowski J (2005) Computationally designed monomers and polymers for molecular imprinting of theophylline and its derivatives. Part I. Polymer 46:7528–7542
15. Pavel D, Lagowski J (2005) Computationally designed monomers and polymers for molecular imprinting of theophylline - part II. Polymer 46:7543–7556
16. Pavel D, Lagowski J, Lepage CJ (2006) Computationally designed monomers for molecular imprinting of chemical warfare agents - Part V. Polymer 47:8389–8399
17. Dineiro Y, Menendez MI, Blanco-Lopez MC, Lobo-Castanon MJ, Miranda-Ordieres AJ, Tunon-Blanco P (2005) Computational approach to the rational design of molecularly imprinted polymers for voltammetric sensing of homovanillic acid. Anal Chem 77:6741–6746
18. Dineiro Y, Menendez MI, Blanco-Lopez MC, Lobo-Castanon MJ, Miranda-Ordieres AJ, Tunon-Blanco P (2006) Computational predictions and experimental affinity distributions for a homovanillic acid molecularly imprinted polymer. Biosens Bioelectron 22:364–371
19. Del Sole R, Lazzoi MR, Arnone M, Della Sala F, Cannoletta D, Vasapollo G (2009) Experimental and computational studies on non-covalent imprinted microspheres as recognition system for nicotinamide molecules. Molecules 14:2632–2649
20. Wu LQ, Li YZ (2004) Study on the recognition of templates and their analogues on molecularly imprinted polymer using computational and conformational analysis approaches. J Mol Recognit 17:567–574
21. Meng Z, Yamazaki T, Sode K (2004) A molecularly imprinted catalyst designed by a computational approach in catalysing a transesterification process. Biosens Bioelectron 20:1068–1075
22. Wu LQ, Sun BW, Li YZ, Chang WB (2003) Study properties of molecular imprinting polymer using a computational approach. Analyst 128:944–949
23. Farrington K, Magner E, Regan F (2006) Predicting the performance of molecularly imprinted polymers. Selectvie extraction of caffeine by molecularly imprinted solid phase extraction. Anal Chim Acta 566:60–68
24. Farrington K, Regan F (2007) Molecularly imprinted sol gel for ibuprofen: an analytical study of the factors influencing selectivity. Biosens Bioelectron 22:1138–1146
25. Liu Y, Wang F, Tan TW, Lei M (2007) Study of the properties of molecularly imprinted polymers by computational and conformational analysis. Anal Chim Acta 581:137–146
26. Lv Y, Lin ZX, Tan TW, Feng W, Qin PY, Li C (2008) Application of molecular dynamics modeling for the prediction of selective adsorption properties of dimethoate imprinting polymer. Sens Actuators, B 133:15–23
27. Lv YQQ, Lin ZX, Feng W, Tan TW (2007) Evaluation of the polymerization and recognition mechanism for phenol imprinting SPE. Chromatographia 66:339–347
28. Azenha M, Kathirvel P, Nogueira P, Fernando-Silva A (2008) The requisite level of theory for the computational design of molecularly imprinted silica xerogels. Biosensors & Bioelectronics 23:1843–1849
29. Spartan'06. Wavefunction, Inc., Irvine, CA
30. Frisch MJ, Trucks GW, Schlegel HB, Scuseria GE, Robb MA, Cheeseman JR, Montgomery JA Jr, Vreven T, Kudin KN, Burant JC, Millam JM, Iyengar SS, Tomasi J, Barone V, Mennucci B, Cossi M, Scalmani G, Rega N, Petersson GA, Nakatsuji H, Hada M, Ehara M, Toyota K, Fukuda R, Hasegawa J, Ishida M, Nakajima T, Honda Y, Kitao O, Nakai H, Klene M, Li X, Knox JE, Hratchian HP, Cross JB, Bakken V, Adamo C, Jaramillo J, Gomperts R, Stratmann RE, Yazyev O, Austin AJ, Cammi R, Pomelli C, Ochterski JW, Ayala PY, Morokuma K, Voth GA, Salvador P, Dannenberg JJ, Zakrzewski VG, Dapprich S, Daniels AD, Strain MC, Farkas O, Malick DK, Rabuck AD, Raghavachari K, Foresman JB, Ortiz JV, Cui Q, Baboul AG, Clifford S, Cioslowski J, Stefanov BB, Liu G, Liashenko A, Piskorz P, Komaromi I, Martin RL, Fox DJ, Keith T, Al-Laham MA, Peng CY, Nanayakkara A, Challacombe M, Gill PMW, Johnson B, Chen W, Wong MW, Gonzalez C, Pople JA (2004) Gaussian 03, Revision C.02. Gaussian Inc, Wallingford
31. Mojica ERE, Autschbach J, Bright FV, Aga DS (2011) Synthesis and evaluation of tetracycline imprinted xerogels: comparison of experiment and computational binding studies. Anal Chim Acta 684:63–71
32. Halgren TA (1992) The representation of van der waals (vdW) interactions in molecular mechanics force fields: potential form, combination rules, and vdW parameters. J Am Chem Soc 114:7827–7843
33. Young DC (2001) Computational chemistry: a practical guide for applying techniques to real world problems. John Wiley & Sons, New York
34. Baggiani C, Anfossi L, Baravalle P, Giavannoli C, Tozzi C (2005) Selectivity features of molecularly imprinted polymers recognisine the carbamate group. Anal Chim Acta 531:199–207
35. Jensen F (2013) Introduction to Computational Chemistry. John Wiley & Sons, West Sussex
36. Friesner RA (2005) Ab initio quantum chemistry: methodology and applications. Proc Natl Acad Sci USA 102:6648–6653
37. Duarte HA, Carvalho S, Paniago EB, Simas AM (1999) Importance of tautomers in the chemical behavior of tetracyclines. J Pharm Sci 88:111–120
38. Atta NF, Hamed MM, Abdel-Mageed AM (2010) Computational investigation and synthesis of a sol–gel imprinted material for sensing application of some biologically active molecules. Anal Chim Acta 667:63–70
39. Becke AD (1993) Density-functional thermochemistry. III. The role of exact exchange. J Chem Phys 98:5648–5653
40. Kowalska A, Stobiecka A, Wysocki S (2009) A computational investigation of the interactions between harmane and the functional monomers commonly used in molecular imprinting. J Mol Struc THEOCHEM 901:88–95
41. Kim M-C, Sim E, Burke K (2011) Communication: avoiding unbound anions in density functional calculations. J Chem Phys 134:171103
42. Curtiss LA, Raghavachari K, Redfern PC, Pople JA (1997) Assessment of Gaussian-2 and density functional theories for the computation of enthalpies of formation. J Chem Phys 106:1063–1079
43. Cossi M, Barone V, Cammi R, Tomasi J (1996) Ab initio study of solvated molecules: a new implementation of the polarizable continuum model. Chem Phys Lett 255:327–335
44. Gholivanda MB, Khodadadiana M, Ahmadib F (2010) Computer aided-molecular design and synthesis of a high selective molecularly imprinted polymer for solid-phase extraction of furosemide from human plasma. Anal Chim Acta 658:225–232
45. Yao J, Li X, Qin W (2008) Computational design and synthesis of molecular imprinted polymers with high selectivity for removal of aniline from contaminated water. Anal Chim Acta 610:282–288
46. Dong CK, Li X, Guo ZC, Qi JY (2009) Development of a model for the rational design of molecular imprinted polymer: computational

approach for combined molecular dynamics/quantum mechanics calculations. Anal Chim Acta 647:117–124
47. Nantasenamat C, Isarankura-Na-Ayudhya C, Naenna T, Prachayasittikul V (2007) Quantitative structure-imprinting factor relationship of molecularly imprinted polymers. Biosens Bioelectron 22:3309–3317
48. Yao JH, Li X, Qin W (2008) Computational design and synthesis of molecular imprinted polymers with high selectivity for removal of aniline from contaminated water. Anal Chim Acta 610:282–288
49. Mukawa T, Goto T, Nariai H, Aoki Y, Imamura A, Takeuchi T (2003) Novel strategy for molecular imprinting of phenolic compounds utilizing disulfide templates. J Pharm Biomed Anal 30:1943–1947
50. Voshell SM, Gagne MR (2005) Rigidified dendritic structures for imprinting chiral information. Organometallics 24:6338–6350
51. Azenha M, Szefczyk B, Loureiro D, Kathirvel P, Cordeiro MNDS, Fernando-Silva A (2011) Molecular dynamics simulations or pregelification mixtures for the production of imprinted xerogels. Langmuir 27:5062–5070